JOURNAL OF Applied Polymer SCIENCE

Special Issue: Bio-based Packaging

Guest Editors: José M. Lagarón, Amparo López-Rubio, and María José Fabra
Institute of Agrochemistry and Food Technology of the Spanish Council for Scientific Research

EDITORIAL

Bio-based Packaging
J. M. Lagarón, A. López-Rubio and M. J. Fabra, *J. Appl. Polym. Sci.* 2015, DOI: 10.1002/app.42971

REVIEWS

Active edible films: Current state and future trends
C. Mellinas, A. Valdés, M. Ramos, N. Burgos, M. D. C. Garrigós and A. Jiménz, *J. Appl. Polym. Sci.* 2015, DOI: 10.1002/app.42631

Vegetal fiber-based biocomposites: Which stakes for food packaging applications?
M.-A. Berthet, H. Angellier-Coussy, V. Guillard and N. Gontard, *J. Appl. Polym. Sci.* 2015, DOI: 10.1002/app.42528

Enzymatic-assisted extraction and modification of lignocellulosic plant polysaccharides for packaging applications
A. Martínez-Abad, A. C. Ruthes and F. Vilaplana, *J. Appl. Polym. Sci.* 2015, DOI: 10.1002/app.42523

RESEARCH ARTICLES

Combining polyhydroxyalkanoates with nanokeratin to develop novel biopackaging structures
M. J. Fabra, P. Pardo, M. Martínez-Sanz, A. Lopez-Rubio and J. M. Lagarón, *J. Appl. Polym. Sci.* 2015, DOI: 10.1002/app.42695

Production of bacterial nanobiocomposites of polyhydroxyalkanoates derived from waste and bacterial nanocellulose by the electrospinning enabling melt compounding method
M. Martínez-Sanz, A. Lopez-Rubio, M. Villano, C. S. S. Oliveira, M. Majone, M. Reis and J. M. Lagarón, *J. Appl. Polym. Sci.* 2015, DOI: 10.1002/app.42486

Bio-based multilayer barrier films by extrusion, dispersion coating and atomic layer deposition
J. Vartiainen, Y. Shen, T. Kaljunen, T. Malm, M. Vähä-Nissi, M. Putkonen and A. Harlin, *J. Appl. Polym. Sci. 2*015, DOI: 10.1002/app.42260

Film blowing of PHBV blends and PHBV-based multilayers for the production of biodegradable packages
M. Cunha, B. Fernandes, J. A. Covas, A. A. Vicente and L. Hilliou, *J. Appl. Polym. Sci.* 2015, DOI: 10.1002/app.42165

On the use of tris(nonylphenyl) phosphite as a chain extender in melt-blended poly(hydroxybutyrate-*co*-hydroxyvalerate)/clay nanocomposites: Morphology, thermal stability, and mechanical properties
J. González-Ausejo, E. Sánchez-Safont, J. Gámez-Pérez and L. Cabedo, *J. Appl. Polym. Sci.* 2015, DOI: 10.1002/app.42390

Characterization of polyhydroxyalkanoate blends incorporating unpurified biosustainably produced poly(3-hydroxybutyrate-*co*-3-hydroxyvalerate)
A. Martínez-Abad, L. Cabedo, C. S. S. Oliveira, L. Hilliou, M. Reis and J. M. Lagarón, *J. Appl. Polym. Sci.* 2015, DOI: 10.1002/app.42633

Modification of poly(3-hydroxybutyrate-*co*-3-hydroxyvalerate) properties by reactive blending with a monoterpene derivative
L. Pilon and C. Kelly, *J. Appl. Polym. Sci.* 2015, DOI: 10.1002/app.42588

Poly(3-hydroxybutyrate-*co*-3-hydroxyvalerate) films for food packaging: Physical–chemical and structural stability under food contact conditions
V. Chea, H. Angellier-Coussy, S. Peyron, D. Kemmer and N. Gontard, *J. Appl. Polym. Sci.* 2015, DOI: 10.1002/app.41850

JOURNAL OF
Applied Polymer
SCIENCE

Special Issue: Bio-based Packaging

Guest Editors: José M. Lagarón, Amparo López-Rubio, and María José Fabra
Institute of Agrochemistry and Food Technology of the Spanish Council for Scientific Research

Impact of fermentation residues on the thermal, structural, and rheological properties of polyhydroxy(butyrate-*co*-valerate) produced from cheese whey and olive oil mill wastewater
L. Hilliou, D. Machado, C. S. S. Oliveira, A. R. Gouveia, M. A. M. Reis, S. Campanari, M. Villano and M. Majone, *J. Appl. Polym. Sci.* 2015, DOI: 10.1002/app.42818

Synergistic effect of lactic acid oligomers and laminar graphene sheets on the barrier properties of polylactide nanocomposites obtained by the in situ polymerization pre-incorporation method
J. Ambrosio-Martín, A. López-Rubio, M. J. Fabra, M. A. López-Manchado, A. Sorrentino, G. Gorrasi and J. M. Lagarón, *J. Appl. Polym. Sci.* 2015, DOI: 10.1002/app.42661

Antibacterial poly(lactic acid) (PLA) films grafted with electrospun PLA/allyl isothiocyanate fibers for food packaging
H. H. Kara, F. Xiao, M. Sarker, T. Z. Jin, A. M. M. Sousa, C.-K. Liu, P. M. Tomasula and L. Liu, *J. Appl. Polym. Sci.* 2015, DOI: 10.1002/app.42475

Poly(L-lactide)/ZnO nanocomposites as efficient UV-shielding coatings for packaging applications
E. Lizundia, L. Ruiz-Rubio, J. L. Vilas and L. M. León, *J. Appl. Polym. Sci.* 2015, DOI: 10.1002/app.42426

Effect of electron beam irradiation on the properties of polylactic acid/montmorillonite nanocomposites for food packaging applications
M. Salvatore, A. Marra, D. Duraccio, S. Shayanfar, S. D. Pillai, S. Cimmino and C. Silvestre, *J. Appl. Polym. Sci.* 2015, DOI: 10.1002/app.42219

Preparation and characterization of linear and star-shaped poly L-lactide blends
M. B. Khajeheian and A. Rosling, *J. Appl. Polym. Sci.* 2015, DOI: 10.1002/app.42231

Mechanical properties of biodegradable polylactide/poly(ether-block-amide)/thermoplastic starch blends: Effect of the crosslinking of starch
L. Zhou, G. Zhao and W. Jiang, *J. Appl. Polym. Sci.* 2015, DOI: 10.1002/app.42297

Interaction and quantification of thymol in active PLA-based materials containing natural fibers
I. S. M. A. Tawakkal, M. J. Cran and S. W. Bigger, *J. Appl. Polym. Sci.* 2015, DOI: 10.1002/app.42160

Graphene-modified poly(lactic acid) for packaging: Material formulation, processing, and performance
M. Barletta, M. Puopolo, V. Tagliaferri and S. Vesco, *J. Appl. Polym. Sci.* 2015, DOI: 10.1002/app.42252

Edible films based on chia flour: Development and characterization
M. Dick, C. H. Pagno, T. M. H. Costa, A. Gomaa, M. Subirade, A. De O. Rios and S. H. Flóres, *J. Appl. Polym. Sci.* 2015, DOI: 10.1002/app.42455

Influence of citric acid on the properties and stability of starch-polycaprolactone based films
R. Ortega-Toro, S. Collazo-Bigliardi, P. Talens and A. Chiralt, *J. Appl. Polym. Sci.* 2015, DOI: 10.1002/app.42220

Bionanocomposites based on polysaccharides and fibrous clays for packaging applications
A. C. S. Alcântara, M. Darder, P. Aranda, A. Ayral and E. Ruiz-Hitzky, *J. Appl. Polym. Sci.* 2015, DOI: 10.1002/app.42362

Hybrid carrageenan-based formulations for edible film preparation: Benchmarking with kappa carrageenan
F. D. S. Larotonda, M. D. Torres, M. P. Gonçalves, A. M. Sereno and L. Hilliou, *J. Appl. Polym. Sci.* 2015, DOI: 10.1002/app.42263

JOURNAL OF
Applied Polymer
SCIENCE

Special Issue: Bio-based Packaging

Guest Editors: José M. Lagarón, Amparo López-Rubio, and María José Fabra
Institute of Agrochemistry and Food Technology of the Spanish Council for Scientific Research

Structural and mechanical properties of clay nanocomposite foams based on cellulose for the food packaging industry
S. Ahmadzadeh, J. Keramat, A. Nasirpour, N. Hamdami, T. Behzad, L. Aranda, M. Vilasi and S. Desobry, *J. Appl. Polym. Sci.* 2015, DOI: 10.1002/app.42079

Mechanically strong nanocomposite films based on highly filled carboxymethyl cellulose with graphene oxide
M. El Achaby, N. El Miri, A. Snik, M. Zahouily, K. Abdelouahdi, A. Fihri, A. Barakat and A. Solhy, *J. Appl. Polym. Sci.* 2015, DOI: 10.1002/app.42356

Production and characterization of microfibrillated cellulose-reinforced thermoplastic starch composites
L. Lendvai, J. Karger-Kocsis, Á. Kmetty and S. X. Drakopoulos, *J. Appl. Polym. Sci.* 2015, DOI: 10.1002/app.42397

Development of bioplastics based on agricultural side-stream products: Film extrusion of *Crambe abyssinica*/wheat gluten blends for packaging purposes
H. Rasel, T. Johansson, M. Gällstedt, W. Newson, E. Johansson and M. Hedenqvist, *J. Appl. Polym. Sci.* 2015, DOI: 10.1002/app.42442

Influence of plasticizers on the mechanical and barrier properties of cast biopolymer films
V. Jost and C. Stramm, *J. Appl. Polym. Sci.* 2015, DOI: 10.1002/app.42513

The effect of oxidized ferulic acid on physicochemical properties of bitter vetch (*Vicia ervilia*) protein-based films
A. Arabestani, M. Kadivar, M. Shahedi, S. A. H. Goli and R. Porta, *J. Appl. Polym. Sci.* 2015, DOI: 10.1002/app.42894

Effect of hydrochloric acid on the properties of biodegradable packaging materials of carboxymethylcellulose/poly(vinyl alcohol) blends
M. D. H. Rashid, M. D. S. Rahaman, S. E. Kabir and M. A. Khan, *J. Appl. Polym. Sci.* 2015, DOI: 10.1002/app.42870

JOURNAL OF Applied Polymer SCIENCE

Poly(L-lactide)/ZnO nanocomposites as efficient UV-shielding coatings for packaging applications

Erlantz Lizundia,[1] Leire Ruiz-Rubio,[1] José Luis Vilas,[1,2] Luis Manuel León[1,2]
[1]Macromolecular Chemistry Research Group (LABQUIMAC), Department of Physical Chemistry, Faculty of Science and Technology, University of the Basque Country (UPV/EHU), Leioa 48940, Spain
[2]Basque Center for Materials, Applications and Nanostructures (BCMaterials), Parque Tecnológico de Bizkaia, Ed. 500, Derio 48160, Spain
Correspondence to: E. Lizundia (E-mail: erlantz.liizundia@ehu.eus)

ABSTRACT: Poly(L-lactide) (PLLA)/ZnO nanocomposites have been developed as efficient UV-shielding coatings for packaging applications. ZnO have been selected as the most suitable UV-shielding material over 10 different metallic nanoparticles. Results reveal a nucleating effect of ZnO in which PLLA crystallization half time is reduced from 7.4 to 4.7 min with only 0.05 wt % ZnO. UV–vis spectroscopy confirms the UV-shielding effect in PLLA/ZnO nanocomposites, where the ultraviolet spectrum is blocked by 61.2% for a concentration as low as 0.45 vol %, while the 95.9% of the visible radiation passes through the material. A schematic representation explaining obtained UV-shielding effect is constructed based on the *photon mean free path* reduction as ZnO concentration increases. Water contact angle increased from 81° up to 91° for the 5 wt % nanocomposite, which would result beneficial in view to develop materials for packaging applications. Dynamic mechanical analysis exhibits a T_g increase with nanoparticle loading arising from the chain confinement caused by the presence of ZnO interacting surfaces. © 2015 Wiley Periodicals, Inc. J. Appl. Polym. Sci. **2016**, *133*, 42426.

KEYWORDS: biomaterials; composites; nanoparticles; nanowires and nanocrystals; optical properties; packaging

Received 4 April 2015; accepted 29 April 2015
DOI: 10.1002/app.42426

INTRODUCTION

The burnout of fossil resources that deals our civilization makes imperative the development of ecofriendly materials with lower energy consumption and environmental impact. In this regard, the improvement of the functional properties of biopolymers that would match the required properties for nowadays applications offer us the possibility of replacing current petroleum-based plastics by biodegradable and renewable polymers,[1] avoiding the use of nonbiodegradable materials such as polystyrene (PE), polyethylene terephthalate (PET), and polypropylene (PP). Polylactides are one of the most promising bioplastics due to their economically feasible industrial production, high transparency, printability, inherent physicochemical characteristics, renewable aspect, and thermoplastic character.[1,2] The presence of an asymmetric carbon in its structure results in different isomeric forms of polylactides,[3] being the semicrystalline poly (L-lactide) (PLLA) the most interesting one because its tunable biodegradability and mechanical properties.[4]

One of the main pathways toward the sustainable development would be the development of PLLA-based parts for packaging industry, where nonbiodegradable materials for short-term use applications are mainly employed. In order to compete with commercial thermoplastic currently used for packaging applications, one of the main drawbacks that need to be faced is the high permeability of PLLA to ultraviolet (UV) light,[2] which dramatically affects the food quality. Indeed, it is proven that lipids, flavors, vitamins, and pigments undergo degradation reactions when exposed to light (oxidation of fats, formation of aldehydes/methyl ketones/free amino acids, loss of vitamin C, discoloration, and so on).[5] In this sense, to prevent the photodegradation of food and preserve them during the storage, it is essential to improve the poor UV light barrier properties of polylactides.

In this hypothesis, an efficient cost-effective approach to address this matter would arise from the addition of fillers in which the dispersed phase should act as strong UV absorbing element. Zinc oxide (ZnO) is a functional n-type semiconductor with a band gap of 3.37 eV which up to date has been used for purposes such as solar energy conversion, electrostatic dissipative coatings, chemical sensors, hybrid solar cells, etc.[6–8] Zinc oxide particles are also being currently utilized in sunscreens and sunblock formulations.[9,10] ZnO-based sunscreens have the advantage over chemical-based sunscreens that they avoid the possible

Additional Supporting Information may be found in the online version of this article.

skin irritation and allergies derived from the use of other UV-protecting chemicals. Accordingly, the addition of environmentally friendly zinc oxide to PLLA would confer high film transparency in the visible range (λ between 400 and 800 nm) and absorb most of the UV light ($\lambda < 400$ nm), especially the UV-B light (λ between 315 and 280 nm), which is the most energetic component of natural UV light.[11]

For effective UV-filtering purposes, nanometric particles are desired, since elements with diameters smaller than one-tenth of the visible light wavelength are free from light scattering,[12] which make ZnO nanoparticles especially interesting. Another important aspect concerning those nanoparticles is their ability to increase antimicrobial resistance to its hosting matrix due to the presence of reactive oxygen species (OH^-) and Zn^{2+} ions when nanoparticles are in contact with water,[13,14] which would further improve the functional properties of polymers for packaging applications.

In this work, PLLA/ZnO nanocomposite films with concentrations up to 5 wt % have been fabricated by solvent-precipitation followed by compression molding. Because of their strong UV absorption behavior, photostability, and safety as denoted by American Food and Drug Administration (FDA) approval,[15] ZnO nanoparticles have been selected to develop PLLA-based nanocomposite films for packaging applications. Functional properties of nanocomposites have been evaluated by UV–vis spectroscopy, water contact angle (WCA) measurements, and dynamic mechanical analysis (DMA).

EXPERIMENTAL

Starting Materials

PLLA of number-average molecular weight (M_n) 120,000 g/mol were kindly supplied by Purac Biochem (The Netherlands). Chloroform was purchased from LabScan and methanol was purchased by Panreac. All the nanoparticles have been kindly purchased by L'Urederra technological center (Spain).

Sample Preparation

Samples have been prepared by solvent-precipitation followed by compression molding. First, ZnO nanoparticles were homogeneously suspended in chloroform ($CHCl_3$) via mild-sonication (20% output for 1 min, Vibra-Cell^{TM} CV 334) and they were added to previously dissolved PLLA to obtain nanocomposites with 1 wt % concentration. Another sonication step (5 min) has been applied to dispersions before precipitating them in an excess of cold methanol, which ensures a homogeneous distribution of zinc oxide within the polymer matrix. After drying the resulting materials for 48 h at 60°C in a vacuum-oven, films with a thickness of 150 μm were fabricated in a hydraulic hot press by compression molding at 200°C for 4 min under a pressure of 150 MPa followed by water-quenching (nearly amorphous specimens were obtained).

Differential Scanning Calorimetry

The thermal behavior of samples was determined using a *Mettler Toledo DSC 822e* calorimeter under nitrogen atmosphere (30 mL/min). Samples of 8 mg were sealed in an aluminum pan, heated from 0 to 200°C at a rate of 10°C/min and held at 200°C for 2 min to remove previous thermal history. Then, samples have been cooled to $T_c = 130$°C at 50°C/min and held at this temperature for 50 min to ensure that crystallization process is completed. A subsequent heating scan at 10°C/min was applied from −20°C to the samples in order to determine the thermal transitions (T_g, ΔH_{cc}, and ΔH_m). The crystalline fraction X_c (%) attributable to the PLLA crystallization during the corresponding heat treatment was determined as follows:[16]

$$X_c(\%) = \frac{\Delta H_f - \Delta H_{cc}}{\Delta H_f{}^0 \cdot W_m} \cdot 100 \tag{1}$$

where ΔH_f and ΔH_{cc} are, respectively, the enthalpy of fusion and cold crystallization of the samples determined on the DSC and W_m is the PLLA matrix weight fraction in the composite sample. $\Delta H_f^0 = 106$ J/g was taken as the heat of fusion of an infinitely thick PLLA crystal.[17]

UV–Vis Spectroscopy

UV–vis absorption spectra were recorded with a Shimadzu MultiSpec-1501 spectrophotometer. Total transmittance experiments have been analyzed in the range of 190–800 nm with a sampling interval of 1 nm and 25 accumulations. UV–vis spectra of metallic nanoparticles have been measured by dispersing nanoparticles in distilled water at a concentration of 0.1 mg/mL under mild sonication conditions (20% output for 5 min, Vibra-Cell^{TM} CV 334). UV–vis spectra of neat PLLA and its nanocomposite counterparts have been collected from ∼12-μm-thick films in transmission mode (see Supplementary Information, Figure S2; the representative profilometry data for PLLA/ZnO nanocomposite films).

Contact Angle Measurements

Water was used as the probe liquid for the determination of hydrophobicity at the nanocomposite surface. Measurements were carried out by sessile drop method (2 μL per drop at a rate of 2 μL/s) using a Neurtek Instruments OCA 15 EC at room temperature. The average values were calculated using six measurements of each composition.

Dynamic Mechanic Analysis

DMA was performed on a DMA/SDTA861 analyzer (Mettler-Toledo) in tensile mode. Specimens of 150 μm, 4 mm wide, and 5.5 mm long were cut from compression-molded sheets. Curves displaying storage modulus (E_0) and the energy loss (tan δ) were recorded as a function of temperature at a heating rate of 3°C/min, a frequency of 1 Hz and force amplitude of 1 N.

RESULTS AND DISCUSSION

UV-Shielding of Raw Metallic Nanoparticles

It is well-known that semiconductor nanoparticles, such as TiO_2, ZnO, CeO_2, Fe_2O_3, and CdS, absorb UV light because of their electronic structures, characterized by a filled valence band and an empty conduction band.[18] In this framework, in order to evaluate which nanoparticle absorbs UV radiation to a larger extent, as shown in Figure 1, UV–vis transmittance spectroscopy has been carried out for 10 different materials. Since the transmittance of a sample (T) could be defined as the relative number of photons that pass through sample (I) under an incident light (I_0), i.e,. $T = I/I_0$, a transmittance close to 100% denotes a completely transparent film to the incident light. The ideal UV-

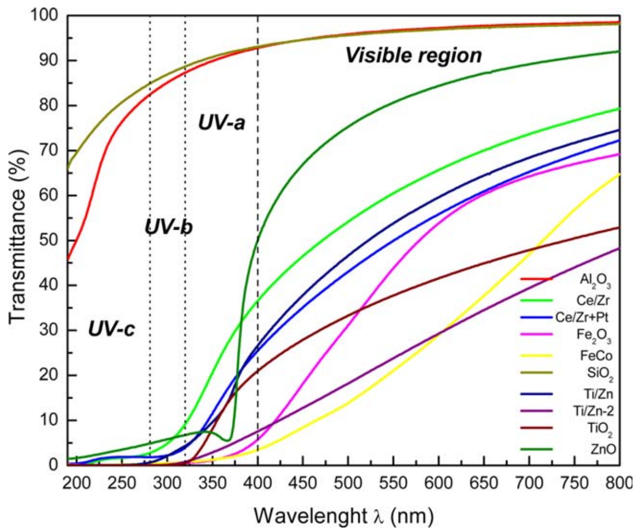

Figure 1. UV–vis transmittance spectra of metallic nanoparticles. [Color figure can be viewed in the online issue, which is available at wileyonlinelibrary.com.]

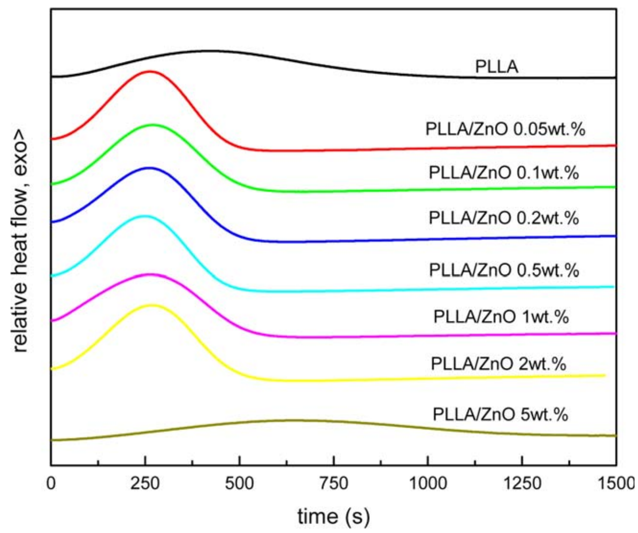

Figure 2. DSC isothermal crystallization traces obtained at $T_c = 130°C$ after quenching PLLA/ZnO nanocomposites from the melt. [Color figure can be viewed in the online issue, which is available at wileyonlinelibrary.com.]

blocking element should present a transmittance of 0% at wavelengths bellow 400 nm and a complete transparency (transmittance of 100%) at wavelengths exceeding 400 nm. According to this statement, among all the studied nanoparticles, ZnO seems to be more effective UV-protecting agent, since they look black in the UV spectrum ($T \sim 7\%$) and rather transparent in the visible region (T ranging from 50 to 90%). This sharp change is due to a process of electron excitation called band-gap absorption, which absorbs light in the UV region. More precisely, the UV–vis absorption spectrum of ZnO presents a strong exciton absorption band centered at 366 nm, which is 9 nm blue shifted compared to the absorption spectrum of bulk zinc oxide.

On the basis of their broad UV absorption range (as shown in Figure 1), strong photostability (the UV absorption capacity does not decrease over time), and safety as denoted by FDA approval,[15] in this work, wurtzite ZnO nanoparticles (as denoted by wide-angle X-ray diffraction pattern shown in Supplementary Information, Figure S3) have been chosen to produce PLLA-based UV-absorbing films.

PLA/ZnO Crystallization Behavior

It is well known that PLLA, as a stereoregular polymer, is able to develop a partial crystallinity when is heat-treated at temperatures between glass transition (T_g) and melting point (T_m).[19] For that purpose, isothermal crystallizations of PLLA/ZnO nanocomposites have been carried out to understand how the presence of ZnO affects the resulting crystallization ability of polymer matrix. Figure 2 shows the isothermal crystallization exotherms of PLLA-based nanocomposites containing up to 5 wt % ZnO nanoparticles obtained at a crystallization temperature of $T_c = 130°C$, while Table I summarizes the crystallization parameters achieved during DSC scan.

In this framework, crystallization half time ($t_{1/2}$) could be used to understand crystallization kinetics of our materials, while crystallinity degree (X_c) could be employed to determine the extent of this process. Additionally, in polymer-based nanocomposites, the T_g value gives us information about the confinement effect induced by the reinforcing phase. It can be observed that even a low amount such as 0.05 wt % is enough to speed up the matrix crystallization since lower times are required for the completion bell-shaped curve. In fact, 15–30 nm wide and 60–110 nm long rod-shaped ZnO nanoparticles (as shown by transmission electron microscopy image at a 140,000× magnification in Supplementary Information, Figure S4) are acting as efficient nucleating agents as illustrated by the reduction of $t_{1/2}$ from 7.4 to 4.7 min with the addition of only 0.05 wt %. This nucleation effect has been widely reported for polymer-based nanocomposites such as Nylon-6/ZnO,[20] PVA/CNT,[21] PP/$CaCO_3$,[22] and PET/MMT.[23] For such a low concentration of 0.05 wt %, this reduction in crystallization time is significantly greater than those previously reported. For instance, Brussiere *et al.* found that silane-treated ZnO nanoparticles delay both cold- and melt-crystallization of PLLA by six times.[24]

Table I. Obtained Isothermal Crystallization Parameters ($t_{1/2}$ and X_c) and Glass Transition Temperature (T_g) for PLLA/ZnO Nanocomposites

ZnO content	0 wt %	0.05 wt %	0.1 wt %	0.2 wt %	0.5 wt %	1 wt %	2 wt %	5 wt %
$t_{1/2}$ (min)	7.4	4.7	4.6	4.4	4.1	4.4	4.5	10.9
T_g (°C)	59.8	59.7	62.6	63.6	65.7	61.3	57.7	57.8
X_c (%)	53.5	55.9	53.4	57.6	54	55.1	62.5	53.1

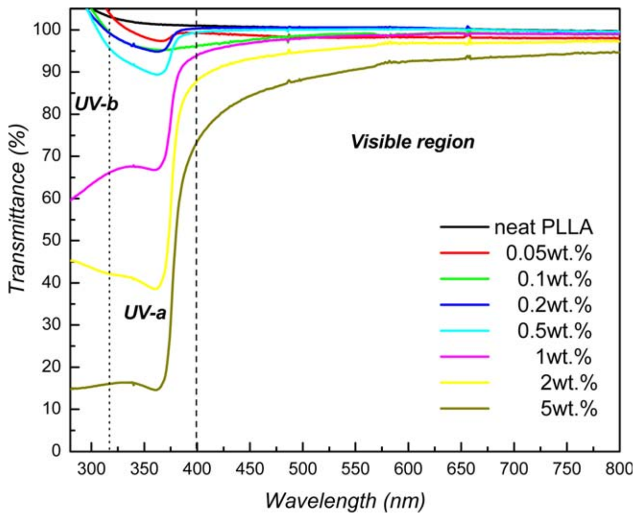

Figure 3. UV–vis transmittance spectra of PLLA/ZnO nanocomposites. [Color figure can be viewed in the online issue, which is available at wileyonlinelibrary.com.]

Further addition of nanoparticles does not induce faster crystallization kinetics, obtaining a concentration range of 0.05–2 wt % in which $t_{1/2}$ comprised between 4.1 and 4.7 min. Moreover, for the 5 wt % nanocomposite, the high nanoparticle density reduces the efficiency of ZnO to boost the matrix crystallization, hindering the formation of ordered crystalline regions and resulting in a $t_{1/2}$ of 10.9 min. The existence of a critical concentration in which a reduction of nucleation surfaces occurs has been previously demonstrated for PLLA/CNT nanocomposites.[25] The increase in T_g for 59.8°C for neat polymer to 65.7°C for its 0.5 wt % nanocomposite counterpart could be attributed to the confinement of PLLA chains caused by the presence of ZnO surfaces.[25] Murariu *et al*. prepared nanocomposites containing both neat ZnO and silane-treated ZnO nanoparticles and they found that the addition of those nanoparticles slightly decreases glass transition temperature of polymer matrix.[26] They attributed this lowering of the T_g to the formation of lactic acid (LA) monomers and oligomers during the fabrication. So, solvent-precipitation followed by compression molding could be seen as an efficient approach to develop PLLA/ZnO nanoparticles since thermal degradation of matrix is prevented. This confining effect induced by ZnO surfaces may delay the relatively quick structural relaxation of polylactides when they are used at room temperature, because the achieved chain-conformation changes would be reduced,[27] which would allow us to develop reliable materials.

The fact that X_c remains nearly constant at 53–57% for all the concentrations suggest that irrespectively of the presence of ZnO, the amount developed crystalline domains is quite similar for the entire composition range. The reduction of the crystallization time is accompanied with an increased T_g for ZnO concentrations up to 0.5 wt %, which suggest a critical concentration in which those nanoparticles result more effective as constraining elements. Those results agree well with Supplementary Information, Figure S1 (FE-SEM images showing ZnO dispersion in PLLA matrix for concentrations of 1 and 5 wt %), where it is proven that ZnO nanoparticles trend to aggregate at concentrations exceeding 1 wt %.

PLLA/ZnO UV–Vis Shielding

Figure 3 shows the UV–vis transmittance spectra of neat PLLA and PLLA/ZnO films with a thickness of 12 μm, while Table II summarizes the amount of transmitted light in the UV and visible regions through PLLA/ZnO nanocomposite films. It could be observed that neat polymer transmits nearly 100% of the light in the studied region. PLLA/ZnO films present a $\lambda_{max} = 366$ nm, which is identical to that obtained for neat nanoparticles. The transparency of a plastic sheeting is determined as the transmission of the light within the 540–560 nm (ASTM D1746-03).[28] As shown in Table II, all samples are characterized by high transparency properties. Indeed, nanocomposite films containing up to 2 wt % ZnO are in the range of the average transparency of food packaging films, which is usually found close to 95%,[29] while their UV-shielding effect is notably larger than that of neat Poly(ethylene terephthalate) (PET), which is widely used as packaging material. In fact, the continuous addition of ZnO results in a systematic decrease of the transmitted light in the region bellow 375 nm. PLLA/ZnO film with a concentration of 2 wt % (0.45 v/v) is able to block around the 57% of UV-B light (280–315 nm), which is the most energetic component of natural light, while absorbs nearly 61% of UV-A light (400–315 nm).

As shown in Supplementary Information, Figure S1, nanocomposites with concentrations up to 1 wt % exhibit uniform ZnO dispersion within the matrix, which would avoid possible dichroism effects arising from nanoparticle orientation (different colors are achieved at the parallel and perpendicular directions).[30] This homogeneous nanoparticle distribution would confer improved optical properties to PLLA/ZnO films. According to Rayleigh scattering, the light loss by scattering steeply increases with particle size,[31] yielding a notable reduction in the transparency of the films together with a whitening effect as particle size/aggregation degree increases. In this sense, the reduction on the visible-light transmission (or optical transparency) from *ca* 100% for film containing 0.5–90.6 wt % for its 5 wt % nanocomposite counterpart denotes a nonuniform dispersion of ZnO nanoparticles within the polymer host, which is in

Table II. Amount of Transmitted Light (%) in the UV Region (360 nm) and Visible Region (540–560 nm) Through PLLA/ZnO Films

	Wavelength	
ZnO concentration (wt %)	360 nm	540–560 nm
0	100	100
0.05	97.7	98.2
0.1	95.6	99.1
0.2	94.9	100
0.5	89.5	100
1	67.3	98.1
2	38.8	95.9
5	14.8	90.6

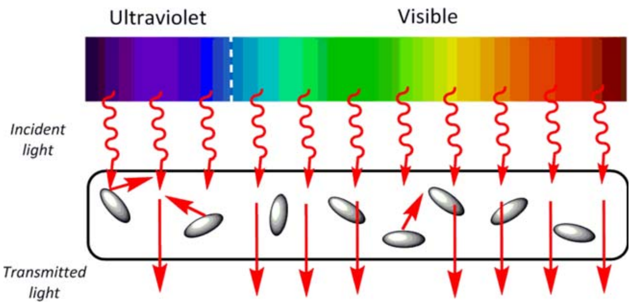

Figure 4. Schematic representation showing the UV-shielding effect in PLLA/ZnO nanocomposite films. [Color figure can be viewed in the online issue, which is available at wileyonlinelibrary.com.]

agreement with FE-SEM images shown in Supplementary Information, Figure S1.

To the best of our knowledge, this work reports for the first time the development of transparent nanocomposite films with strong UV protection up to 85% based on naturally available materials. For instance, previous works have shown UV-protection behavior with visible transmittances of about 40% for ABS/ZnO nanocomposites,[32] 75% and 55% for 1 wt % nanocomposites with untreated and surface-treated ZnO nanoparticles,[26] total transmittance of 85% for bacterial cellulose/ acrylic resins,[33] and increase in opacity of PLA films from 15 to 25% with a ZnO concentration of 3 wt %.[34] Furthermore, it is interesting to note that zinc oxide nanoparticles have been homogeneously dispersed within hydrophobic PLLA for concentrations up to 1 wt % by solvent-precipitation method with no need of dispersants such as triethoxy caprylsilane.[24] This improvement in the fabrication method could lead nanocomposite films with improved functional properties since it has been found that such dispersants interfere several physicochemical processes such as crystallization.[24]

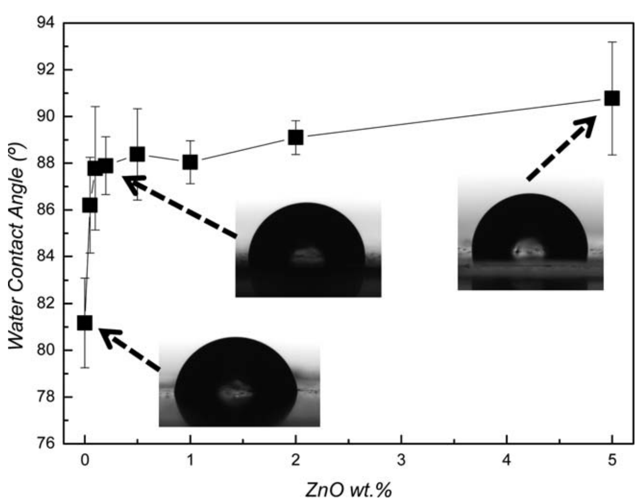

Figure 5. Water contact angle values of PLLA/ZnO nanocomposites as a function of ZnO concentration. Representative images of a water drop at the surface of neat PLLA and nanocomposite films containing 0.2 and 5 wt % are shown.

According to obtained experimental results, a schematic representation of UV-shielding effect in PLLA/ZnO nanocomposite films is constructed as shown in Figure 4. Polymer host is represented as a chamfered rectangle in which ZnO nanoparticles (grey ellipses) are randomly distributed. When nanocomposite film is stroked by an incident light (wavy red lines), the visible radiation almost completely passes through the material because ZnO nanoparticles are transparent for wavelengths larger than ~380 nm. On the contrary, ultraviolet spectrum is blocked depending on the nanoparticle concentration. ZnO nanoparticles create a physical barrier for the transmission of UV light because they behave as a labyrinth that UV light cannot cross. Increasing nanoparticle concentration, the *photon mean free path* decreases, photons travel across the film with increased hindrance, resulting in a reduction on the UV-light transmission from 97.5% for the nanocomposite containing 0.05–38.8 wt % for its 2 wt % (or 0.45 v/v) counterpart. In overall, those results demonstrate that PLLA/ZnO nanocomposites could effectively be used as a coating for packaging industry, where the products need to be preserved from UV-light until they reach final consumers.

Surface Hydrophobicity

Water contact angle (WCA) measurements were carried out to further characterize the functional properties of PLLA/ZnO films for packaging applications. As shown in Figure 5, neat PLLA shows a WCA of to 81°, which is in good agreement with previously reported values.[35] With the addition of ZnO nanoparticles, this contact angle is increased up to 91° for the 5 wt % nanocomposite, denoting an increased surface hydrophobicity induced by the presence of metallic nanoparticles, as previously obtained for several biopolymer/ZnO nanocomposites.[13] *A priori* it would be expected that the hydrolytic degradation of PLLA could be delayed due to the restricted water diffusion into the material. This wettability reduction could be further used toward the development of self-cleaning polylactide-based films for packaging applications.[36]

Dynamic Mechanical Properties

It has been previously shown that ZnO could be effectively used as a reinforcing element to improve the tensile strength of polymers while maintaining their flexibility.[37] In this sense, DMA has been carried out to analyze the mechanical properties of obtained materials. Figure 6 shows the normalized storage modulus (E') and tan δ curves of PLLA/ZnO nanocomposites over the temperature range of 20–100°C.

Neat polymer shows a sharp glass transition at 66°C as denoted by the marked decrease in E'. Glass transition temperature of nanocomposites slightly increases with nanoparticle concentration by 2°C, while tan δ values remain almost unchanged. Nanocomposites present a rather stiffer behavior than neat polymer, especially at temperatures above T_g, where the E' modulus of the specimen containing 0.2 wt % is increased by ~4 times at 100°C in regard to neat PLLA. This increase in the rigidity of the composite may be related to the restriction of the mobility of the polymer host at the nanoparticle surface,[38] which is usually referred as chain-confinement.[4,16] It is noteworthy that the main changes are obtained at a concentration of 1

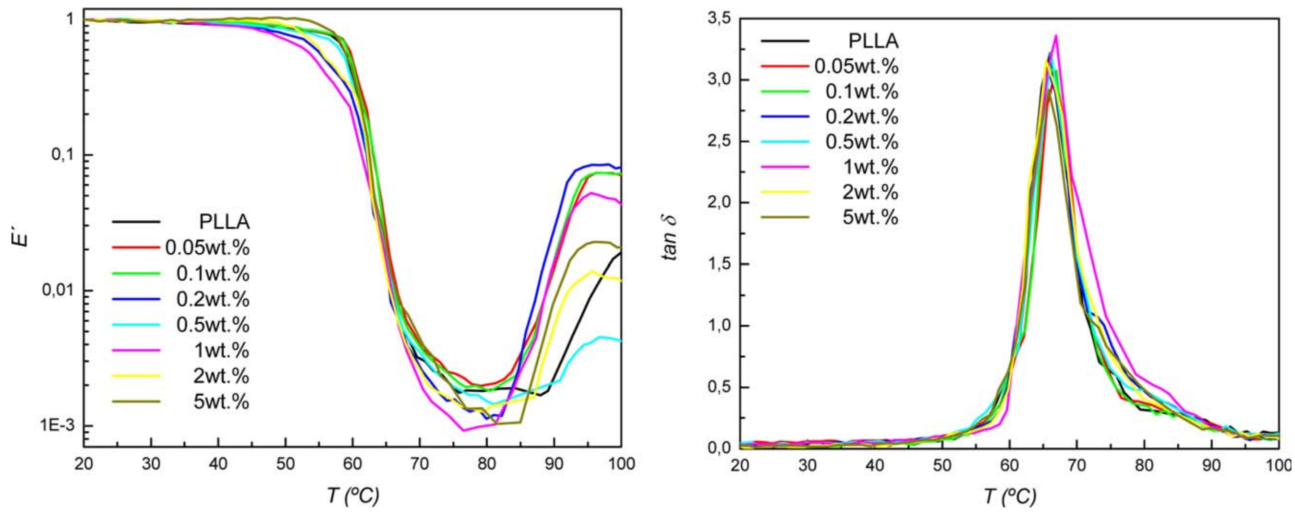

Figure 6. Dynamic mechanical storage modulus vs temperature (left) and tan δ vs temperature (right) plots for neat PLLA and its nanocomposites. [Color figure can be viewed in the online issue, which is available at wileyonlinelibrary.com.]

wt %, suggesting that larger concentration yields nanoparticle aggregation (as confirmed by FE-SEM micrographs, Supplementary Information, Figure S1), decreasing the matrix/reinforcement contact area.[39] Those results agrees well with abovementioned DSC data, where it has been found the existence of a critical concentration in which ZnO nanoparticles behave as effective constraining elements.

CONCLUSIONS

In this work, transparent and colorless UV-shielding PLLA/ZnO films have been developed. UV–vis spectroscopy tests demonstrate that ZnO results especially suitable as UV-shielding material among metallic nanoparticles. DSC results demonstrate that crystallization half time is reduced from 7.4 to 4.7 for a 0.05 wt % concentration given by the strong nucleating effect of ZnO surfaces.

Nanocomposite films with a thickness of 12 μm with a concentration as low as 0.45 vol % is able to block 61.2% of UV light while maintaining a transparency of 95.9% in the visible region. It is hypothesized that as ZnO concentration increases nanoparticles create a physical barrier for the transmission of UV light, yielding a reduction in the *photon mean free path*. The obtained increase in surface hydrophobicity with ZnO concentration would further improve their functional properties for packaging applications since it would allow the fabrication of self-cleaning polylactide-based films. Additionally, a chain confinement effect induced by the numerous interacting ZnO surfaces has been found by both DSC and DMA experiments. Obtained experimental findings through this work lead the way for the development of efficient and cost-effective transparent UV-shielding coatings based on a renewable polymer and natural filler to be used in packaging industry.

ACKNOWLEDGMENTS

E. L. thanks the University of the Basque Country (UPV/EHU) for a postdoctoral fellowship. We gratefully acknowledge Corbion-Purac for the kind donation of PLLA. Technical and human support provided by SGIker (UPV/EHU, MICINN, GV/EJ, EGEF, and ESF) is gratefully acknowledged. Authors thank the Basque Country Government for finnancial support (Ayudas para apoyar las actividades de los grupos de investigación del sistema universitario vasco, IT718-13).

REFERENCES

1. Drumright, R. E.; Gruber, P. R.; Henton, D. E. *Adv. Mat.* **2000**, *12*, 1841.
2. Auras, R.; Harte, B.; Selke, S. *Macromol. Biosci.* **2004**, *4*, 835.
3. Meaurio, E.; Martinez de Arenaza, I.; Lizundia, E.; Sarasua, J. R. *Macromolecules* **2009**, *42*, 5717.
4. Lizundia, E.; Petisco, S.; Sarasua, J. R. *J. Mech. Behav. Biomed. Mater.* **2013**, *17*, 242.
5. Turhan, K. N.; Sahbaz, F. *Polym. Int.* **2001**, *50*, 1138.
6. Wang, Z. L.; Song, J. *Science* **2006**, *312*, 242.
7. Jung, J.; Yoon, Y. J.; He, M.; Lin, Z. *J. Polym. Sci. Part B: Polym. Phys.* **2014**, *52*, 1641.
8. Sosa, O.; Noguez, C.; Barrera, R. G. *J. Phys. Chem. B* **2003**, *107*, 6269.
9. Serpone, N.; Dondi, D.; Albini, A. *Inorg. Chim. Acta* **2007**, *360*, 794.
10. Weir, A.; Westerhoff, P.; Fabricius, L.; Hristovski, K.; von Goetz, N. *Environ. Sci. Technol.* **2012**, *46*, 2242.
11. Li, Y. Q.; Fu, S. Y.; Mai, Y. W. *Polymer* **2006**, *47*, 2127.
12. Novak, B. M. *Adv. Mat.* **1993**, *5*, 422.
13. Kanmani, P.; Rhim, J. W. *Carbohyd. Polym.* **2014**, *106*, 190.
14. Lipovsky, A.; Nitzan, Y.; Gedanken, A.; Lubart, R. *Nanotechnology* **2011**, *22*, 105101 (5 pp).
15. Sambandan, D. R.; Ratner, D. *J. Am. Acad. Dermatol.* **2011**, *64*, 748.
16. del Rio, J.; Etxeberria, A.; Lopez-Rodriguez, N.; Lizundia, E.; Sarasua, J. R. *Macromolecules* **2010**, *43*, 4698.

17. Sarasua, J. R.; Prud'homme, R. E.; Wisniewski, M.; Le Borgne, A.; Spassky, N. *Macromolecules* **1998**, *31*, 3895.
18. Kubacka, A.; Fernández-García, M.; Colón, G. *Chem. Rev.* **2011**, *112*, 1555.
19. Lizundia, E.; Vilas, J. L.; León, L. M. *Carbohyd. Polym.* **2015**, *123*, 256.
20. Zheng, J.; Siegel, R. W.; Toney, C. G. *J. Polym. Sci. Part B: Polym. Phys.* **2003**, *41*, 1033.
21. Coleman, J. N.; Cadek, M.; Ryan, K. P.; Fonseca, A.; Nagy, J. B.; Blau, W. J.; Ferreira, M. S. *Polymer* **2006**, *47*, 8556.
22. Chan, C. M.; Wub, J.; Lia, J. X.; Cheung, Y. K. *Polymer* **2002**, *43*, 2981.
23. Calcagno, C. I. W.; Mariani, C. M.; Teixeira, S. R.; Mauler, R. S. *Polymer* **2007**, *48*, 966.
24. Bussiere, P. O.; Therias, S.; Gardette, J. L.; Murariu, M.; Dubois, P.; Baba, M. *J. Phys. Chem. C* **2012**, *35*, 12301.
25. Lizundia, E.; Oleaga, A.; Salazar, A.; Sarasua, J. R. *Polymer* **2012**, *53*, 2412.
26. Murariu, M.; Doumbia, A.; Bonnaud, L.; Dechief, A. L.; Paint, Y.; Ferreira, M.; Campagne, C.; Devaux, E.; Dubois, P. *Biomacromolecules* **2011**, *5*, 1762.
27. Lizundia, E.; Sarasua, J. R. *Macromol. Symp.* **2012**, *321–322*, 118.
28. ASTM-D1746-03. Standard Test Method for Transparency of Plastic Sheeting, American Society for Testing and Materials, West Conshohocken, PA **2003**, *8.01*, 398.
29. Auras, R. A.; Lim, L. T.; Selke, S. E. M.; Tsuji, H., Eds., Poly(lactic acid): Synthesis, Structures, Properties, Processing, and Applications; John Wiley & Sons: New York, **2010**.
30. Caseri, W. *Macromol. Rapid. Comm.* **2000**, *21*, 705.
31. Althues, H.; Henle, J.; Kaskel, S. *Chem. Soc. Rev.* **2007**, *36*, 1454.
32. Rodriguez-Tobias, H.; Morales, G.; Rodriguez-Fernandez, O.; Acuña, P. *Macromol. Symp.* **2013**, *325–326*, 147.
33. Nogi, M.; Handa, K.; Nakagaito, A. N.; Yano, H. *Appl. Phys. Lett.* **2005**, *87*, 243110.
34. Pantani, R.; Gorrasi, G.; Vigliotta, G.; Murariu, M.; Dubois, P. *Eur. Polym. J.* **2013**, *49*, 3471.
35. Lizundia, E.; Sarasua, J. R.; D'Angelo, F.; Orlacchio, A.; Martino, S.; Kenny, J. M.; Armentano, I. *Macromol. Biosci.* **2012**, *12*, 870.
36. Sas, I.; Gorga, R. E.; Joines, J. A.; Thoney, K. A. *J. Polym. Sci. Part B: Polym. Phys.* **2012**, *50*, 824.
37. Chen, Y. Y.; Kuo, C. C.; Chen, B. Y.; Chiu, P. C.; Tsai, P. C. *J. Polym. Sci. Part B: Polym. Phys.* **2015**, *53*, 262.
38. Elen, K.; Murariu, M.; Peeters, R.; Dubois, Ph.; Mullens, J.; Hardy, A.; Van Bael, M. K. *Polym. Adv. Technol.* **2012**, *23* 1422.
39. Kim, I. H.; Jeong, Y. G. *J. Polym. Sci. Part B: Polym. Phys.* **2010**, *48*, 850.